Advances in Nano Research, *Vol. 15, No. 1 (2023) 75-89*
https://doi.org/10.12989/anr.2023.15.1.075

Bishop theory and longitudinal vibration of nano-beams by two-phase local/nonlocal elasticity

Reza Nazemnezhad**[1], Roozbeh Ashrafian*[1] and Alireza Mirafzal[2b]

[1]*School of Engineering, Damghan University, Damghan, Iran*
[2]*Faculty of Mechanical Engineering, Semnan University, Semnan, Iran*

(*Received January 31, 2022, Revised December 27, 2022, Accepted January 17, 2023*)

Abstract. In this paper, Bishop theory performs longitudinal vibration analysis of Nano-beams. Its governing equation, due to integrated displacement field and more considered primarily effects compared with other theories, enjoys fully completed status, and more reliable results as well. This article aims to find how Bishop theory and Two-phase elasticity work together. In other words, whether Bishop theory will be compatible with Two-phase local/nonlocal elasticity. Hamilton's principle is employed to derive governing equation of motion, and then the 6th order of Generalized Differential Quadrature Method (GDQM) as a constructive numerical method is utilized to attain the discretized two-phase formulation. To acquire a proper verification procedure, exact solution is prepared to be compared with current results. Furthermore, the effects of key parameters on the objective are investigated.

Keywords: axial vibration; bishop theory; generalised differential quadrature method (GDQM); nano-beams; two-phase local/nonlocal elasticity

1. Introduction

Behavior and mechanical properties of nanoscale systems as a crucial field of study have been found a particular value among researchers. Huge region of application in diverse fields such as biotechnology, thermal generators, Micro/Nano Electro-Mechanical Systems (MEMS/NEMS), and Micro/Nano-sensors and Nano-motors are mentionable (Bergman 1968). Theoretical results having been relied on classical continuum theories have always been more convenient in contrast to other methods. Thus, new definition or modification of preliminary theories, including strain gradient theory, nonlocal elastic theory, nonlocal strain gradient theory, and couple stress theory have been considered by numerous researchers. Some literature associated with above-mentioned theories are eventually cited (Bergman 1968, Lim *et al*. 2015, Eringen 1983, 1984, Eringen and Wegner 2003, Lam *et al*. 2003, Fleck 1994). Defined stress in nonlocal theories is an independent variable of strain domain throughout. Eringen and Wegner (2003) by an integral formula based on the definition stated in the prior sentence and its simplification presented a constructive theory. However, differential form of Eringen's nonlocal elastic theory have attracted more interest to analyze mechanical problems. Fernandez-saez *et al*. (2016) through an analysis devoted to bending of Euler–Bernoulli beams stated that differential type is completely different from Eringen integral equation. Furthermore, compound of differential form of this theory and strain gradient theory can be an integrated procedure to achieve both nonlocal and strain gradient effects. To reach further perception, more comprehensive studies are suggested (Lei *et al*. 2013, Reddy 2007, Thai 2012, Lu *et al*. 2017, Shen 2016, Zhu and Li 2017). The result of the mechanics of nanostructures having been studied by differential nonlocal have shown that nonlocal parameter surging leads to more softening effect although differential form of nonlocal elasticity enjoys some paradoxical influences. Challamel *et al*. (2014) in a paper, investigated the one-dimensional Eringen's nonlocal elasticity based on simple models. It was stated that the model may be nonself-adjoint and that it can produce an unexpected stiffening effect for a cantilever's natural frequency with increasing Eringen's small length scale coefficient. Appuzo *et al*. (2017) through an investigation of free vibrations of Nano-beams compared stress-driven nonlocal integral model (SDM) with Eringen differential law (EDM) and the gradient elasticity theory (GradEla). To create more constructive method, Eringen's combination of local and nonlocal has been used by researchers, for example, Wang *et al*. (2016) by an analytical study analyzed bending of Euler-Bernoulli beams statically using Eringen's two-phase local/nonlocal model. Zhu *et al*. (2017) utilized Eringen's two-phase integral model to analyze the buckling problem of Euler-Bernoulli beams. Khaniki (2018) stated that differential form of Eringen's nonlocal theory does not enjoy reasonable performance in analyzing small-scale structures. Accordingly, a comprehensive study on vibration of double-layered Nano-beam was presented within the framework of Eringen's two-phase local/nonlocal. Two-phase elasticity theory without contradictions in modelling vibrations of Nano-beams as well as development of proper solution procedures in domain of corresponding differential

*Corresponding author, M.S,
E-mail: R.ashrafian@du.ac.ir
**Co-corresponding author, Associate Professor,
E-mail: rnazemnezhad@du.ac.ir

ISSN: 2287-237X (Print), 2287-2388 (Online)

equations that in comparison with common nonlocal differential theory eliminated contradictions and consequently provides integral form of results in accordance with differential one. Moreover, through comparing results of two-phase theory and nonlocal, it can be said that in addition to elimination of contradictions, softening effect of nonlocal parameter consideration appears with more intensity in two-phase domain (with a quantity close to zero) that this enjoys more discrepancy in higher modes. Some researchers through employing conventional theories have attempted to form higher order theories to study Micro and Nano-beams behaviors. For example, a non-classical Bernoulli-Euler (BE) beam model developed by Zhang *et al*. (2021) employed a simplified micromorphic elasticity theory. The BL beam model is then formulated by applying the simplified micromorphic theory and employing a variational approach based on Hamilton's principle. Zhang and Gao (2019) in another work presented a non-classical Bernoulli–Euler beam model developed using a reformulated strain gradient elasticity theory that incorporates both couple stress and strain gradient effects. Employing nonlocal theory for FGM vastly in order to enjoy buckling, bending, and vibrational analysis have been an interesting field thus far. To perceive further some related literature (Mirafzal and Fereidoon 2017, Mashat *et al*. 2016, Li and Wang 2012, Besseghier *et al*. 2015, Eltaher *et al*. 2012, Şimşek and Yurtcu 2013, Chaht *et al*. 2015, Jalaei *et al* 2022) are introduced. In recent years, some works associated with Nano-beams and elasticity theory have attracted loads of attention. For instance, Hsu *et al*. (2011) addressed axial vibration of a cracked beam subjected to the transverse magnetic field through nonlocal elasticity theory. In this study one dimensional wave theory is employed and a linear spring as the crack part of the beam is modelled. A novel approach presented by Lin *et al*. (2020) investigates the vibration and buckling analysis of nanobeams with surface stress effects. In this study, the material model is derived in which the bulk core of a beam is assumed to be a single crystalline material. In addition, the beams are assumed to be covered by atomic layers with the crystallographic directions on the top and bottom surfaces. In another outstanding paper by Zhao *et al*. (2020) based on the strain gradient theory a size-dependent axially functional gradient (AFG) flexoelectric Euler-Bernoulli nanobeam model is developed. A modified power-law formula incorporating porosity volume fraction is presented to define material properties of porous AFG nanobeam, and two typical porosity distributions patterns are considered. Further works associated with nanorods and nonlocal theories investigated by several researchers are worth reading (Numanoğlu and Civalek 2019, 2022, Numanoğlu *et al*. 2021, 2018). Nazemnezhad and Shokrollahi (2022) through employing Love-Bishop theory presented an analysis associated with axial frequencies of axially functionally graded material (AFGM) Nano-rods considering surface energy effect. Nazemnezhad and Kamali (2018) studied free axial vibration of (AFG) Nano-rods by Bishop theory. Additionally, the nonlocal theory considering the small scale effect are employed. Büşra Uzun *et al* (2020) investigated axial vibrations of Nano-rods with different boundary conditions. Bishop theory considered to simulate the axial deflection was the main platform. Eringen's nonlocal theory as a size-dependency was considered in this study. Civalek and Numanoğlu (2020) examined nonlocal free vibration of axial rods embedded in elastic medium by utilizing Love–Bishop rod theory with finite element method. The study of both free and time-dependent forced axial vibration simultaneously in single-walled carbon nanotubes subjected to a moving load conducted by Hosseini *et al*. (2019) considered classical theory, along with the Rayleigh and Bishop theories so as to analyze the nonlocal vibrational behaviors of single-walled carbon nanotubes. Consideration of inertia of lateral motions and shear stiffness leads to a comprehensive analysis compared to other basic theories. Therefore, Bishop theory with further assumptions can provide further accurate analysis.

Bishop theory for the first time as an all-embracing platform and two-phase local/nonlocal elasticity are utilized to analyze longitudinal vibration of Nano-beams. Governing equations, in presence of axial and transverse displacements, are derived by means of Hamilton's principle and differential law of two-phase elasticity. Next, The Generalized Differential Quadrature Method (GDQM) is employed to attain the discretized two-phase formulation. In order to obtain confirmations, the reliability of the method, and the result are compared with those presented in literature. Also, the effects of various parameters such as, height, nonlocal factor and local phase fraction coefficient on the natural frequencies are investigated.

2. Problem formulation

Regarding considering the effect not only of the inertia of the lateral motions but also of the shear stiffness, the Bishop's displacement field is given by Eq. (1). The elements in the cross section of the beam located at the coordinates y and z, undergoes the lateral displacements, second and third part of Eq. (1), respectively, along the y and z directions with ν denoting Poisson's ratio. Thus, *U*, *V*, and *W* are the displacement of the Nano-beam in axial and lateral directions, respectively (Rao 2019).

$$U = u(x,t)$$
$$V = -\nu y \frac{\partial u(x,t)}{\partial x} \tag{1}$$
$$W = -\nu z \frac{\partial u(x,t)}{\partial x}$$

And the axial and transverse shear strains can be obtained as (Rao 2019)

$$\varepsilon_{xx} = \frac{\partial U}{\partial x}$$
$$\varepsilon_{yy} = \frac{\partial V}{\partial y} = -\nu \frac{\partial u(x,t)}{\partial x} \tag{2}$$
$$\varepsilon_{zz} = \frac{\partial W}{\partial z} = -\nu \frac{\partial u(x,t)}{\partial x}$$

$$\varepsilon_{xy}=\left(\frac{\partial U}{\partial y}+\frac{\partial V}{\partial x}\right)=-vy\frac{\partial^2 u(x,t)}{\partial x^2}$$
$$\varepsilon_{zx}=\left(\frac{\partial U}{\partial z}+\frac{\partial W}{\partial x}\right)=-vz\frac{\partial^2 u(x,t)}{\partial x^2}$$
$$\varepsilon_{yz}=\left(\frac{\partial W}{\partial y}+\frac{\partial V}{\partial z}\right)=0$$

The stress, normal and shear, induced in the cross section of the beam can be determined using the three-dimensional Hook's law as (Rao 2019)

$$\begin{Bmatrix}\sigma_{xx}\\ \sigma_{yy}\\ \sigma_{zz}\\ \sigma_{xy}\\ \sigma_{yz}\\ \sigma_{zx}\end{Bmatrix}=\frac{E}{(1+\nu)(1-2\nu)}$$
$$\begin{bmatrix}1-\nu & \nu & \nu & 0 & 0 & 0\\ \nu & 1-\nu & \nu & 0 & 0 & 0\\ \nu & \nu & 1-\nu & 0 & 0 & 0\\ 0 & 0 & 0 & \frac{1-2\nu}{2} & 0 & 0\\ 0 & 0 & 0 & 0 & \frac{1-2\nu}{2} & 0\\ 0 & 0 & 0 & 0 & 0 & \frac{1-2\nu}{2}\end{bmatrix}\begin{Bmatrix}\varepsilon_{xx}\\ \varepsilon_{yy}\\ \varepsilon_{zz}\\ \varepsilon_{xy}\\ \varepsilon_{yz}\\ \varepsilon_{zx}\end{Bmatrix} \quad (3)$$

Which *E*, and *G* are elastic modulus, and shear modulus respectively, and substitution of Eq. (2) in Eq. (3) results in

$$\begin{Bmatrix}\sigma_{xx}\\ \sigma_{yy}\\ \sigma_{zz}\\ \sigma_{xy}\\ \sigma_{yz}\\ \sigma_{zx}\end{Bmatrix}=\begin{Bmatrix}E\frac{\partial u(x,t)}{\partial x}\\ 0\\ 0\\ -vGy\frac{\partial^2 u(x,t)}{\partial x^2}\\ 0\\ -vGz\frac{\partial^2 u(x,t)}{\partial x^2}\end{Bmatrix} \quad (4)$$

Nano-beam strain energy is (Rao 2019)

$$\pi=\frac{1}{2}\iiint_V(\sigma_{xx}\varepsilon_{xx}+\sigma_{yy}\varepsilon_{yy}+\sigma_{zz}\varepsilon_{zz}+\sigma_{xy}\varepsilon_{xy}+\sigma_{yz}\varepsilon_{yz}+\sigma_{zx}\varepsilon_{zx})dV \quad (5)$$

As seen above, non-zero quantities are imported into Eq. (5). Axial force, $N(x,t)=\int_A\sigma_{xx}dA$, should be defined and by using Eq. (2), and Eq. (3), Eq. (5) is rewritten as

$$\pi=\frac{1}{2}\int_0^l dx\iint_0^A dA\begin{bmatrix}E\left(\frac{\partial u(x,t)}{\partial x}\right)^2+0+0\\ +\nu^2Gy^2\left(\frac{\partial^2 u(x,t)}{\partial x^2}\right)^2\\ +0+\nu^2Gz^2\left(\frac{\partial^2 u(x,t)}{\partial x^2}\right)^2\end{bmatrix}=\frac{1}{2}\int_0^l\begin{bmatrix}N(x,t)\left(\frac{\partial u(x,t)}{\partial x}\right)\\ +\nu^2GI_p\left(\frac{\partial^2 u(x,t)}{\partial x^2}\right)^2\end{bmatrix}dx \quad (6)$$

The kinetic energy of the beam can be obtained as follow (Rao 2019)

$$T=\frac{1}{2}\int_0^l dx\int_0^A\rho dA\left[\left(\frac{\partial U}{\partial t}\right)^2+\left(\frac{\partial V}{\partial t}\right)^2+\left(\frac{\partial W}{\partial t}\right)^2\right] \quad (7)$$

ρ denotes density, after substitutions

$$T=\frac{1}{2}\int_0^l\rho A\left(\frac{\partial u(x,t)}{\partial t}\right)^2dx+\frac{1}{2}\int_0^l\rho\nu^2I_p\left(\frac{\partial^2 u(x,t)}{\partial x\partial t}\right)^2dx \quad (8)$$

I_p, the polar moment of the inertia of the cross section, is defined by (Rao 2019)

$$I_p=\int_A(y^2+z^2)dA \quad (9)$$

Hamilton's principle is utilized to derive governing equation and boundary conditions.

$$\delta\int_{t_1}^{t_2}(T-\pi+W)\,dt=0 \quad (10)$$

The variation of kinetic energy, strain energy, and the work done by the external forces not considered in this study should be calculated and substituted in Eq. (10), thus the governing equation of motion and corresponding boundary conditions are expressed as

$$\nu^2GI_p\frac{\partial^4 u(x,t)}{\partial x^4}-\nu^2\rho I_p\frac{\partial^4 u(x,t)}{\partial x^2\partial t^2}-\frac{\partial N(x,t)}{\partial x}+\rho A\left(\frac{\partial^2 u(x,t)}{\partial t^2}\right)=0 \quad (11)$$

$$(N(x,t)+\nu^2\rho I_p\left(\frac{\partial^3 u(x,t)}{\partial x\partial t^2}\right)-\nu^2\frac{\partial}{\partial x}(GI_p\frac{\partial^2 u(x,t)}{\partial x^2}))\delta u(x,t)|_0^l+(\nu^2GI_p\frac{\partial^2 u(x,t)}{\partial x^2})\delta(\frac{\partial u(x,t)}{\partial x})|_0^l=0 \quad (12)$$

Note that Eq. (12) is satisfied if the beam is fixed at the ends $x=0$ and $x=l$. If the bar is fixed at the ends, the axial displacement and shear strain will be zero at each end (Rao 2019), thus

$$u(0,t)=0,u(l,t)=0,\frac{d^2u(0,t)}{dx^2}=0,\frac{d^2u(l,t)}{dx^2}=0 \quad (13)$$

3. Two phase elasticity

Two-phase local/nonlocal elasticity shown below comprises local and nonlocal parts. According to Eringen's model (Eringen and Wegner 2003, Eringen 1984), the stress at a point is a function of the strain as the independent variable not only at the related point but also at other points of the domain. The strain and stress fields satisfy the following constitutive integral equation (Naderi *et al.* 2020).

$$T = \zeta D\varepsilon + (1-\zeta)\int_{\bar{V}} B\, D\bar{\varepsilon} d\bar{V} \tag{14}$$

$$B = \frac{1}{2\kappa} e^{-(\frac{DX}{\kappa})}$$
$$DX = |x - \bar{x}| \tag{15}$$

Here T, ζ, D, ε, B, $\bar{V}$, and κ indicate the stress defined through two phase local/nonlocal elasticity, local phase fraction coefficient, elasticity tensor, strain tensor, Kernel function, volume of the domain, and nonlocal factor, respectively. Polyanin and Manzhirov (2008) presented the equal differential of the integral equation with two constitutive boundary conditions (CBC) as follow.

$$S1(x) = S2(x) + C\int_a^b e^{\mu|x-\bar{x}|} Y(\bar{x}) d\bar{x} \tag{16}$$

$$\ddot{S2}(x) + \mu(2C - \mu)S2(x) = \ddot{S1}(x) - \mu^2 S1(x) \tag{17}$$

$$\dot{S2}(a) + \mu S2(a) = \dot{S1}(a) + \mu S1(a) \tag{18}$$

$$\dot{S2}(b) - \mu S2(b) = \dot{S1}(b) - \mu S1(b) \tag{19}$$

Eq. (17) is a differential form of Eq. (16), and being satisfied two additional boundary conditions are essential to have the replacement.

4. Two phase axial force

By using the Eqs. (14), (15) and the primary form of axial force defined earlier, two-phase axial force is written as

$$N = \zeta EA\frac{\partial u}{\partial x} + EA\frac{(1-\zeta)}{2\kappa}\int_0^l e^{-\frac{DX}{\kappa}}(\frac{\partial u}{\partial \bar{x}})d\bar{x} \tag{20}$$

Now, by employing Eqs. (16), (17), and (20) as well as governing equation, the differential form of axial force is derived as below.

$$N = -\zeta EA\kappa^2\frac{\partial^3 u}{\partial x^3} + EA\frac{\partial u}{\partial x} + \nu^2 GI_p\kappa^2\frac{\partial^5 u}{\partial x^5} - \nu^2\rho I_p\kappa^2\frac{\partial^5 u}{\partial x^3\partial t^2} + \rho A\kappa^2\left(\frac{\partial^3 u}{\partial x\partial t^2}\right) \tag{21}$$

Eventually, by substituting Eq. (21) into governing equation, the expected form of governing equation is derived.

$$-\nu^2 GI_p\kappa^2\frac{\partial^6 u}{\partial x^6} + \left(\nu^2 GI_p + \zeta EA\kappa^2\right)\frac{\partial^4 u}{\partial x^4} - EA\frac{\partial^2 u}{\partial x^2} = [-\nu^2\rho I_p\kappa^2\frac{\partial^4}{\partial x^4} + (\nu^2\rho I_p + \rho A\kappa^2)\frac{\partial^2}{\partial x^2} - \rho A]\left(\frac{\partial^2 u}{\partial t^2}\right) \tag{22}$$

And, according to Eqs. (18), (19) and (21) the CBCs of axial force will be obtained as

$$\begin{aligned}&-\nu^2 GI_p\kappa^3\frac{\partial^6 u(0,t)}{\partial x^6} + \nu^2 GI_p\kappa^2\frac{\partial^5 u(0,t)}{\partial x^5}\\ &+\zeta EA\kappa^3\frac{\partial^4 u(0,t)}{\partial x^4} - \zeta EA\kappa^2\frac{\partial^3 u(0,t)}{\partial x^3}\\ &-EA\kappa(1-\zeta)\frac{\partial^2 u(0,t)}{\partial x^2} + (1-\zeta)EA\frac{\partial u(0,t)}{\partial x}\\ &= [-\nu^2\rho I_p\kappa^3\frac{\partial^4}{\partial x^4} + \nu^2\rho I_p\kappa^2\frac{\partial^3}{\partial x^3} + \rho A\kappa^3\frac{\partial^2}{\partial x^2} - \rho A\kappa^2\frac{\partial}{\partial x}](\frac{\partial^2 u(0,t)}{\partial t^2})\end{aligned} \tag{23}$$

$$\begin{aligned}&-\nu^2 GI_p\kappa^3\frac{\partial^6 u(l,t)}{\partial x^6} - \nu^2 GI_p\kappa^2\frac{\partial^5 u(l,t)}{\partial x^5}\\ &+\zeta EA\kappa^3\frac{\partial^4 u(l,t)}{\partial x^4} + \zeta EA\kappa^2\frac{\partial^3 u(l,t)}{\partial x^3}\\ &+EA\kappa(\zeta-1)\frac{\partial^2 u(l,t)}{\partial x^2} + EA(\zeta-1)\frac{\partial u(l,t)}{\partial x}\\ &= \left[-\nu^2\rho I_p\kappa^3\frac{\partial^4}{\partial x^4} - \nu^2\rho I_p\kappa^2\frac{\partial^3}{\partial x^3} + \rho A\kappa^3\frac{\partial^2}{\partial x^2} + \rho A\kappa^2\left(\frac{\partial}{\partial x}\right)\right](\frac{\partial^2 u(l,t)}{\partial t^2})\end{aligned} \tag{24}$$

5. Generalized differential quadrature method (GDQM)

Generalized differential quadrature method (GDQM) has been proposed as a general numerical method to solve high-order differential equations. Based on the sixth-order derivatives GDQM, the r-th order derivative of a function is considered as follow (Bert and Malik 1996, Wang *et al*. 2003, Wu and Liu 2000, Shu and Richards 1992, Quan and Chang 1989, Wu and Liu 2001, Shafiei *et al*. 2017)

$$\begin{aligned}w^{(r)}(x_i) &= \sum_{k=0}^{2} h_{1k}^{(r)}(x_i)w_1^{(k)} + \sum_{j=2}^{N-1} h_{j0}^{(r)}(x_i)w_j + \sum_{k=0}^{2} h_{Nk}^{(r)}(x_i)w_N^{(k)}\\ &= \sum_{k=1}^{N+4} E_{ik}^{(r)}U_k \qquad i = 1,2,\dots,ns\end{aligned} \tag{25}$$

Parameters consisting, r, N, x_i, $h_{j0}^{(r)}$, $h_{1k}^{(r)}$,and $h_{Nk}^{(r)}$ shows the derivative order, the number of sample points, their location, Hermite shape functions for all sample points, Hermite shape functions for rth order derivative at the first sample point, and the last sample point.

$$\left\{E_{ik}^{(r)}\right\}^T = \begin{Bmatrix} h_{10}^{(r)}(x_i), h_{11}^{(r)}(x_i), \\ h_{12}^{(r)}(x_i), h_{20}^{(r)}(x_i), \\ h_{30}^{(r)}(x_i), \dots, \\ h_{(N-1)0}^{(r)}(x_i), h_{N0}^{(r)}(x_i), \\ h_{N1}^{(r)}(x_i), h_{N2}^{(r)}(x_i) \end{Bmatrix} \tag{26}$$

$$U_k = \{U_1, U_2, \dots, U_j, \dots, U_{N+4}\} = \begin{Bmatrix} w_1, w_1^{(1)}, w_1^{(2)}, w_2, w_3, \dots, \\ w_{N-1}, w_N, w_N^{(1)}, w_N^{(2)} \end{Bmatrix} \quad (27)$$

Hermite shape functions are as follow

$$h_{1(i)}(x) = \frac{(x-x_N)^2}{(x_1-x_N)^2}\left(a_{1(i)}x^2 + b_{1(i)}x + c_{1(i)}\right)l_1(x) \qquad i = 0,1,2 \quad (28)$$

$$h_{N(i)}(x) = \frac{(x-x_1)^2}{(x_1-x_N)^2}\left(a_{N(i)}x^2 + b_{N(i)}x + c_{N(i)}\right)l_N(x) \qquad i = 0,1,2 \quad (29)$$

$$h_{j0}(x) = \frac{(x-x_1)^2(x-x_N)^2}{(x_j-x_1)^2(x_j-x_N)^2}l_j(x) \qquad j = 2,3,\dots,N-1 \quad (30)$$

where a_{pi}, b_{pi}, and c_{pi} are given in appendix. Also, $l_j(x)$ is equivalent to the δ_{ij}, Kronecker delta. Also, the weighting coefficients, Lagrangian interpolation for the first derivative, and higher order derivatives, can be expressed as

$$l_j^{(1)}(x_i) = \begin{cases} \dfrac{R^{(1)}(x_i)}{(x_i-x_j)R^{(1)}(x_j)} & i,j = 1,2,\dots,N; i \neq j \\ -\sum\limits_{j=1,\ i\neq j}^{ns} l_j^{(1)}(x_i) & i,j = 1,2,\dots,N \end{cases} \quad (31)$$

$$R^{(1)}(x_i) = \prod_{m=1,\ m\neq i}^{ns}(x_i - x_m) \quad (32)$$

$$l_j^{(r)}(x_i) = \begin{cases} r\left(l_i^{(r-1)}(x_i)l_j^{(1)}(x_i) - \dfrac{l_j^{(r-1)}(x_i)}{(x_i-x_j)}\right) & i,j = 1,\dots,N; i \neq j \\ -\sum\limits_{j=1,\ i\neq j}^{ns} l_j^{(r)}(x_i) & i,j = 1,\dots,N \end{cases} \quad (33)$$

Both equally space model and Chebyshev Gauss Lobatto model could be used, however owing to reliable and quick convergence, the latter, Eq. (34), is utilized.

$$x_i = \frac{L}{2}\left[1 - \cos\left(\frac{(i-1)}{(ns-1)}\pi\right)\right] \quad i = 1,2,\dots,N \quad (34)$$

6. Vibration analysis

To analyze longitudinal vibration of the system, harmonic vibration has been assumed, thus the displacement field can be shaped as shown below

$$U(x,t) = U(x)e^{i\lambda t} \quad (35)$$

In Eq. (35) λ is devoted to the frequency and t shows the time factor. To derive the discretized governing equation in axial direction by utilizing Eqs. (25) and (35) into Eqs. (22), can be the final part to achieve expected results.

Table 1 Material properties

Material Properties	
ρ	1000 (kg/m^3)
ν	0.38
κ/L	0.03~0.07
H/L	0.01~0.05
E	2e9 (Gpa)
L	1 (nm)

$$\begin{aligned} &-\nu^2 GI_p\kappa^2\sum_{k=1}^{N+4}E_{ik}^{(6)}U_k + \left(\nu^2 GI_p + \zeta EA\kappa^2\right)\sum_{k=1}^{N+4}E_{ik}^{(4)}U_k \\ &-EA\sum_{k=1}^{N+4}E_{ik}^{(2)}U_k = [+\nu^2\rho I_p\kappa^2\sum_{k=1}^{N+4}E_{ik}^{(4)}U_k \\ &-\left(\nu^2\rho I_p + \rho A\kappa^2\right)\sum_{k=1}^{N+4}E_{ik}^{(2)}U_k + \rho AU_{i+2}]\lambda^2 \end{aligned} \quad (36)$$

Furthermore, applying Eqs. (25) and (35) into Eqs. (23) and (24) finalize the discrete type of CBCs.

$$\begin{aligned} &-\nu^2 GI_p\kappa^3\sum_{k=1}^{N+4}E_{ik}^{(6)}U_k + \nu^2 GI_p\kappa^2\sum_{k=1}^{N+4}E_{ik}^{(5)}U_k \\ &+\zeta EA\kappa^3\sum_{k=1}^{N+4}E_{ik}^{(4)}U_k - \zeta EA\kappa^2\sum_{k=1}^{N+4}E_{ik}^{(3)}U_k \\ &\qquad - EA\kappa(1-\zeta)U_3 + (1-\zeta)EAU_2 \\ &= [+\nu^2\rho I_p\kappa^3\sum_{k=1}^{N+4}E_{ik}^{(4)}U_k - \nu^2\rho I_p\kappa^2\sum_{k=1}^{N+4}E_{ik}^{(3)}U_k - \rho A\kappa^3U_3 \\ &\qquad + \rho A\kappa^2U_2]\lambda^2 \end{aligned} \quad (37)$$

$$\begin{aligned} &-\nu^2 GI_p\kappa^3\sum_{k=1}^{N+4}E_{ik}^{(6)}U_k - \nu^2 GI_p\kappa^2\sum_{k=1}^{N+4}E_{ik}^{(5)}U_k \\ &+\zeta EA\kappa^3\sum_{k=1}^{N+4}E_{ik}^{(4)}U_k + \zeta EA\kappa^2\sum_{k=1}^{N+4}E_{ik}^{(3)}U_k \\ &\qquad + EA\kappa(\zeta-1)U_{N+4} + EA(\zeta-1)U_{N+3} \\ &= \left[+\nu^2\rho I_p\kappa^3\sum_{k=1}^{N+4}E_{ik}^{(4)}U_k + \nu^2\rho I_p\kappa^2\sum_{k=1}^{N+4}E_{ik}^{(3)}U_k \right. \\ &\qquad \left. - \rho A\kappa^3U_{N+4} - \rho A\kappa^2U_{N+3}\right]\lambda^2 \end{aligned} \quad (38)$$

Eqs. (36), (37), and (38) are formed in a matrix, thus it could be shaped just as below. Eq. (39) shows an eigenvalue problem that results in natural frequencies and mode shapes, all b-subscripted and d-subscripted parameters devoted to boundary and domain respectively.

$$\begin{bmatrix} [K_{bb}]_{6*6} & [K_{bd}]_{6*(ns-2)} \\ [K_{db}]_{(ns-2)*6} & [K_{dd}]_{(ns-2)*(ns-2)} \end{bmatrix}\begin{Bmatrix}\{V_b\}\\ \{V_d\}\end{Bmatrix} - \lambda^2\begin{bmatrix} [M_{bb}]_{6*6} & [M_{bd}]_{6*(ns-2)} \\ [M_{db}]_{(ns-2)*6} & [M_{dd}]_{(ns-2)*(ns-2)} \end{bmatrix}\begin{Bmatrix}\{V_b\}\\ \{V_d\}\end{Bmatrix} = 0 \quad (39)$$

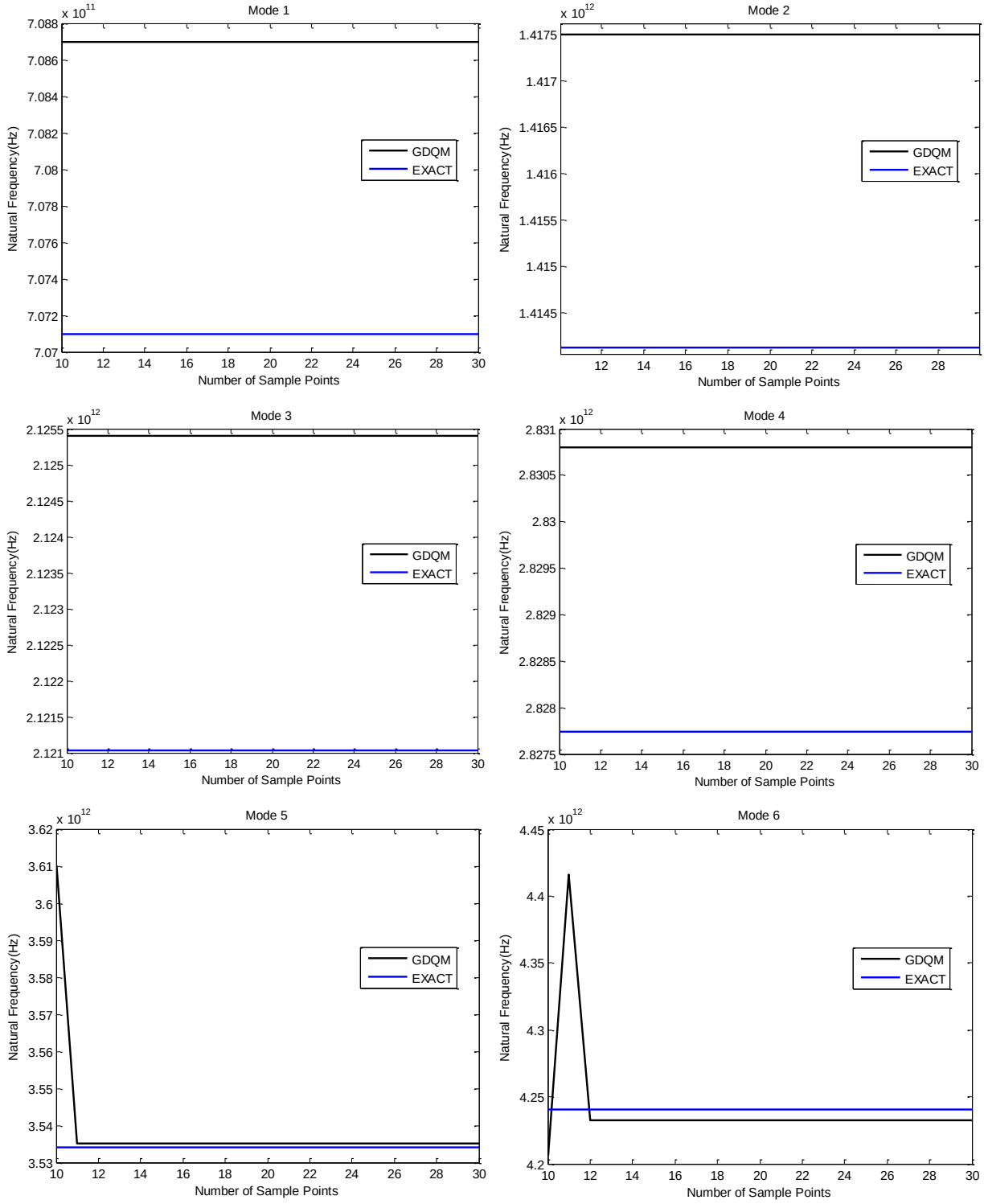

Fig. 1 Convergence of first ten natural frequencies of Bishop theory with $\zeta = 1$, H/L=0.01

7. Numerical results

To realize and achieve a reliable verification the whole process is considered without two-phase local/nonlocal elasticity. In other words, $\zeta = 1$ is assumed. Thus, a reasonable comparison between proposed procedure and the fundamental method presented by Rao (2019) is feasible to be defined. In this part Fig. 1 shown below and comprising 10 portions is illustrated to show how GDQM approach to the exact solution for ten first natural frequencies of the Nano-beam with square cross section. In Table 1 material properties is listed.

Additionally, the formula of natural frequency derived by Rao (2019) based on Bishop theory is mentioned here

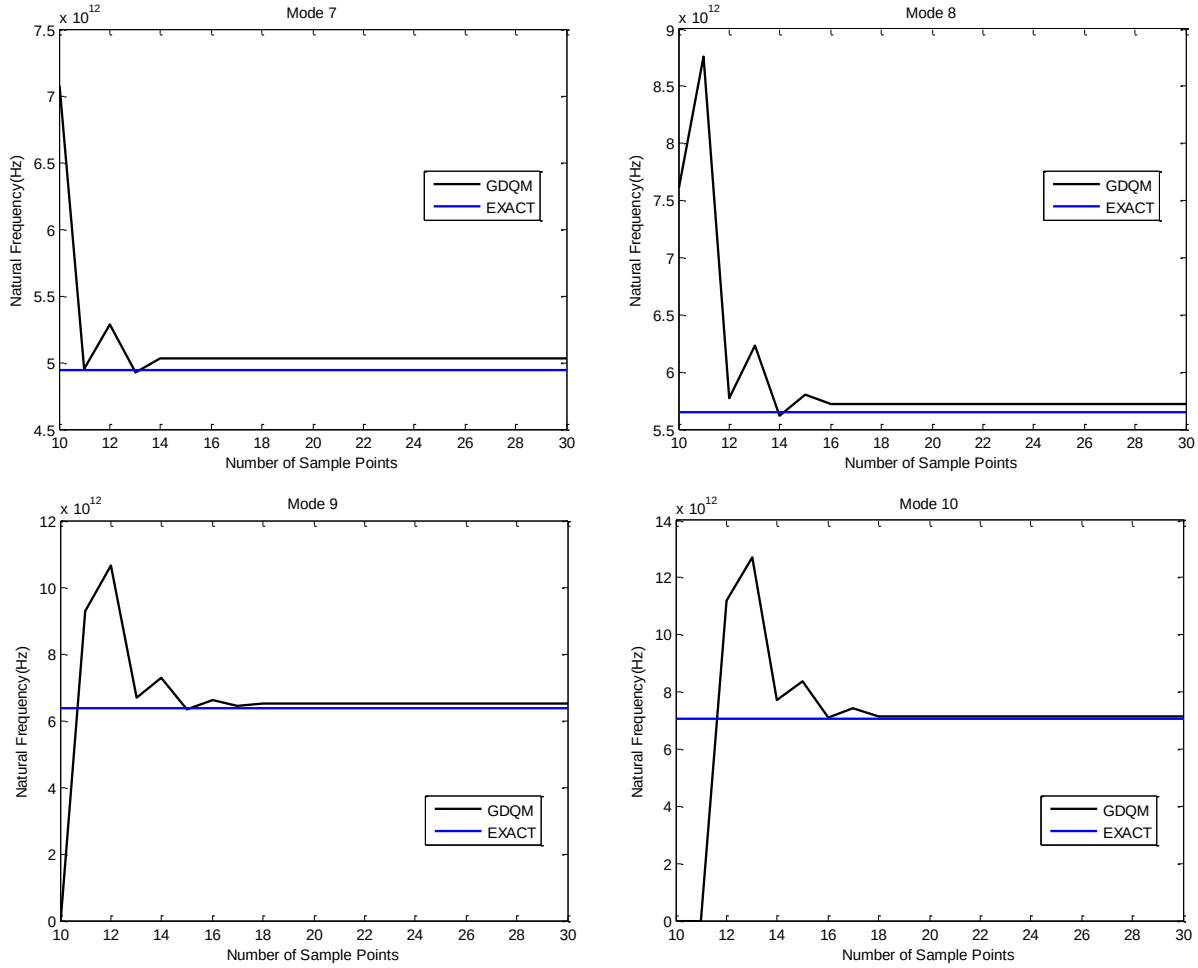

Fig. 1 Continued

$$\omega_n^2 = \frac{n^2\pi^2 E}{\rho l^2}\left(\frac{AEl^2 + \nu^2 GI_p n^2\pi^2}{AEl^2 + \nu^2 EI_p n^2\pi^2}\right) \tag{40}$$

In all parts of the figure, blue lines are devoted to exact solution, and black ones show the convergence path of GDQM. As demonstrated, horizontal axis is devoted to sample points, which is considered with 30 points as upper restriction. Vertical axis is also allocated to natural frequency, which is assumed without non-dimension-alization process. As shown, GDQM with a considerable pace achieve convergence almost at ten sample point for the early orders of natural frequencies. The illustration approved that sixth- order GDQM can be counted as a fast numerical method to achieve reliable solutions.

Moreover, it can be mentioned that nearly five fluctuations are occurred to result in a smooth overlap, and it seems that higher orders of frequencies need to be analyzed with more sample points, for instance, tenth natural frequency's convergence is occurred at almost 20 sample points. Thus, at higher orders convergence is somewhat awkward.

In next portion, there are two series of bar charts and two tables, Figs. 2 and 3, Tables 2 and 3 in which distinct values of *H/L* for various amounts of ζ are considered. Realizing how natural frequency change with changing local phase fraction coefficient and height of cross section is the main aim to present such results. Indeed, existence of table and bar chart alongside could be an integrated status for result presentation. What is clear and describable in Table 2 is that increasing *H/L* for $\zeta = 0.2$ do not result in a particular and clear consequence although a negligible surging tendency is shown for *H/L=0.01* and *H/L=0.02*. Discrepancy for height of cross section in lower cases do not produce a significant effect on natural frequency, but for higher orders of local phase fraction coefficient increasing *H/L* cause a noticeable upward moving of natural frequency. In following bar charts, associated with Table. 3, an integrated vision is illustrated to prepare profound perception. In addition to all details described in prior segment, it can be added that order of natural frequency for each mode shape number is rose smoothly.

In a homogeneous path, impact of surging nonlocal factor with distinct values of local phase fraction coefficient is investigated. Unlike prior consequence, reasonable relation of $\zeta = 0.2$ for all κ/L is distinguishable. As recognizable, except the first natural frequency column, rest of columns for each ζ enjoy a decreasing trend. Likewise, bar charts demonstrate proper outline, and identical results could be obtained.

All defined interval for H/L and κ/L are inserted in 3D

Table 2 Natural Frequencies for distinct values of H/L and ζ, κ/L=0.05

ζ	H/L	MODE SHAPE NUMBER									
		1st	2nd	3rd	4th	5th	6th	7th	8th	9th	10th
	0.01	0.717671	1.394171	2.005844	2.539707	3.007099	3.413715	3.780522	4.111917	4.425617	4.720521
	0.02	0.718771	1.394777	2.007783	2.539354	3.00804	3.41173	3.780279	4.109073	4.425414	4.718477
0.2	0.03	0.710561	1.371201	1.979737	2.491161	2.96133	3.350219	3.727732	4.049281	4.377519	4.667047
	0.04	0.731734	1.421848	2.043972	2.58755	3.060353	3.473473	3.843894	4.182146	4.49864	4.811194
	0.05	0.7305	1.419249	2.044551	2.566562	3.090265	3.399123	3.961866	4.029186	4.575878	4.721294
	0.01	0.725632	1.419387	2.064977	2.652021	3.192919	3.690057	4.162969	4.611128	5.051454	5.478308
	0.02	0.727133	1.421313	2.068431	2.654507	3.196664	3.692005	4.166075	4.612036	5.053492	5.477866
0.4	0.03	0.727956	1.421284	2.069687	2.653022	3.196449	3.687825	4.163385	4.604895	5.047614	5.467232
	0.04	0.726989	1.415938	2.064931	2.640998	3.185258	3.674625	4.141844	4.58187	5.026612	5.438243
	0.05	0	0.87231	1.712891	2.226454	2.969239	3.324413	4.012445	4.293761	4.893164	5.222395
	0.01	0.732227	1.44199	2.119997	2.757406	3.3665	3.945359	4.511566	5.059757	5.606181	6.141395
	0.02	0.733973	1.444571	2.124322	2.76129	3.371752	3.949213	4.51633	5.062238	5.609011	6.141032
0.6	0.03	0.734993	1.445328	2.126366	2.761415	3.372794	3.946848	4.514208	5.055395	5.601387	6.127219
	0.04	0.735664	1.444667	2.127201	2.758152	3.373545	3.937228	4.507923	5.0413	5.586519	6.10334
	0.05	0.747012	1.41633	2.16818	2.69097	3.438139	3.847328	4.5545	4.967374	5.587092	6.050457
	0.01	0.738091	1.463167	2.172436	2.857803	3.530545	4.1841	4.833992	5.470462	6.109285	6.737867
	0.02	0.740121	1.466419	2.177763	2.863172	3.53755	4.190009	4.840816	5.474974	6.113675	6.738548
0.8	0.03	0.741133	1.467464	2.179673	2.864316	3.53831	4.187836	4.838045	5.466867	6.103324	6.720592
	0.04	0.742175	1.467514	2.181914	2.861788	3.538141	4.182466	4.831101	5.4524	6.085473	6.692116
	0.05	0.74423	1.468356	2.186417	2.859566	3.537938	4.178519	4.822974	5.434964	6.063825	6.656762
	0.01	0.743483	1.483372	2.222922	2.954083	3.686555	4.40912	5.135243	5.851272	6.572647	7.284133
	0.02	0.745829	1.487345	2.229416	2.961131	3.695524	4.417458	5.14457	5.858368	6.579345	7.286766
1	0.03	0.746887	1.48847	2.231641	2.961952	3.696856	4.415156	5.141172	5.848999	6.566528	7.265121
	0.04	0.746599	1.49182	2.227984	2.962613	3.698492	4.407956	5.133689	5.83228	6.544934	7.231125
	0.05	0.748653	1.489979	2.233405	2.970037	3.685868	4.400984	5.121574	5.810002	6.516035	7.186814

Table 3 Natural Frequencies for distinct values of κ/L and ζ, H/L=0.01

ζ	κ/L	MODE SHAPE NUMBER									
		1st	2nd	3rd	4th	5th	6th	7th	8th	9th	10th
	0.03	0.715544	1.41534	2.088259	2.721614	3.314085	3.858892	4.363214	4.823968	5.252699	5.647002
	0.04	0.716895	1.406604	2.051259	2.635909	3.163519	3.632406	4.057008	4.438898	4.794099	5.121999
0.2	0.05	0.717671	1.394171	2.005844	2.539707	3.007099	3.413715	3.780522	4.111917	4.425617	4.720521
	0.06	0.717889	1.378562	1.954872	2.440393	2.857096	3.217489	3.546467	3.848759	4.141705	4.422533
	0.07	0.717566	1.360336	1.90093	2.343304	2.72011	3.048433	3.354405	3.641364	3.925387	4.201766
	0.03	0.719624	1.427068	2.114618	2.771842	3.399572	3.991353	4.555238	5.086891	5.59808	6.08426
	0.04	0.722836	1.424643	2.092982	2.715715	3.297913	3.83678	4.346647	4.825896	5.290108	5.734967
0.4	0.05	0.725632	1.419387	2.064977	2.652021	3.192919	3.690057	4.162969	4.611128	5.051454	5.478308
	0.06	0.728018	1.411682	2.032811	2.58644	3.093726	3.561431	4.011913	4.443874	4.873972	5.294729
	0.07	0.73	1.40195	1.998492	2.522982	3.004901	3.453435	3.891519	4.316111	4.743011	5.163039
	0.03	0.722887	1.437183	2.138597	2.818699	3.480341	4.116836	4.736859	5.334269	5.920881	6.489631
	0.04	0.727684	1.440561	2.131517	2.790677	3.424597	4.028519	4.616111	5.182124	5.741543	6.286458
0.6	0.05	0.732227	1.44199	2.119997	2.757406	3.3665	3.945359	4.511566	5.059757	5.606181	6.141395
	0.06	0.736514	1.441703	2.105509	2.722683	3.311956	3.873641	4.42739	4.966727	5.508039	6.040298
	0.07	0.740545	1.439965	2.08939	2.689103	3.263761	3.814544	4.361735	4.897256	5.437258	5.969399

Table 3 Continued

ζ	κ/L	MODE SHAPE NUMBER									
		1st	2nd	3rd	4th	5th	6th	7th	8th	9th	10th
	0.03	0.725721	1.446447	2.161272	2.86362	3.558	4.237303	4.910457	5.569335	6.225578	6.869638
	0.04	0.731949	1.455346	2.168189	2.862456	3.545573	4.210389	4.869527	5.514152	6.158602	6.79177
0.8	0.05	0.738091	1.463167	2.172436	2.857803	3.530545	4.1841	4.833992	5.470462	6.109285	6.737867
	0.06	0.74414	1.469978	2.17469	2.851471	3.515787	4.161522	4.805961	5.438208	6.074712	6.701641
	0.07	0.750081	1.475874	2.17552	2.844728	3.502717	4.143335	4.784775	5.414975	6.050712	6.677212
	0.03	0.728274	1.455172	2.183055	2.907089	3.633195	4.353599	5.077222	5.793902	6.514956	7.228487
	0.04	0.735835	1.469379	2.203521	2.931719	3.661774	4.383902	5.109474	5.826249	6.547938	7.260615
1	0.05	0.743483	1.483372	2.222922	2.954083	3.686555	4.40912	5.135243	5.851272	6.572647	7.284133
	0.06	0.751199	1.497033	2.24104	2.974043	3.70771	4.429887	5.155765	5.870717	6.591406	7.301707
	0.07	0.758961	1.510256	2.257754	2.99166	3.725648	4.446981	5.172219	5.886033	6.605934	7.315174

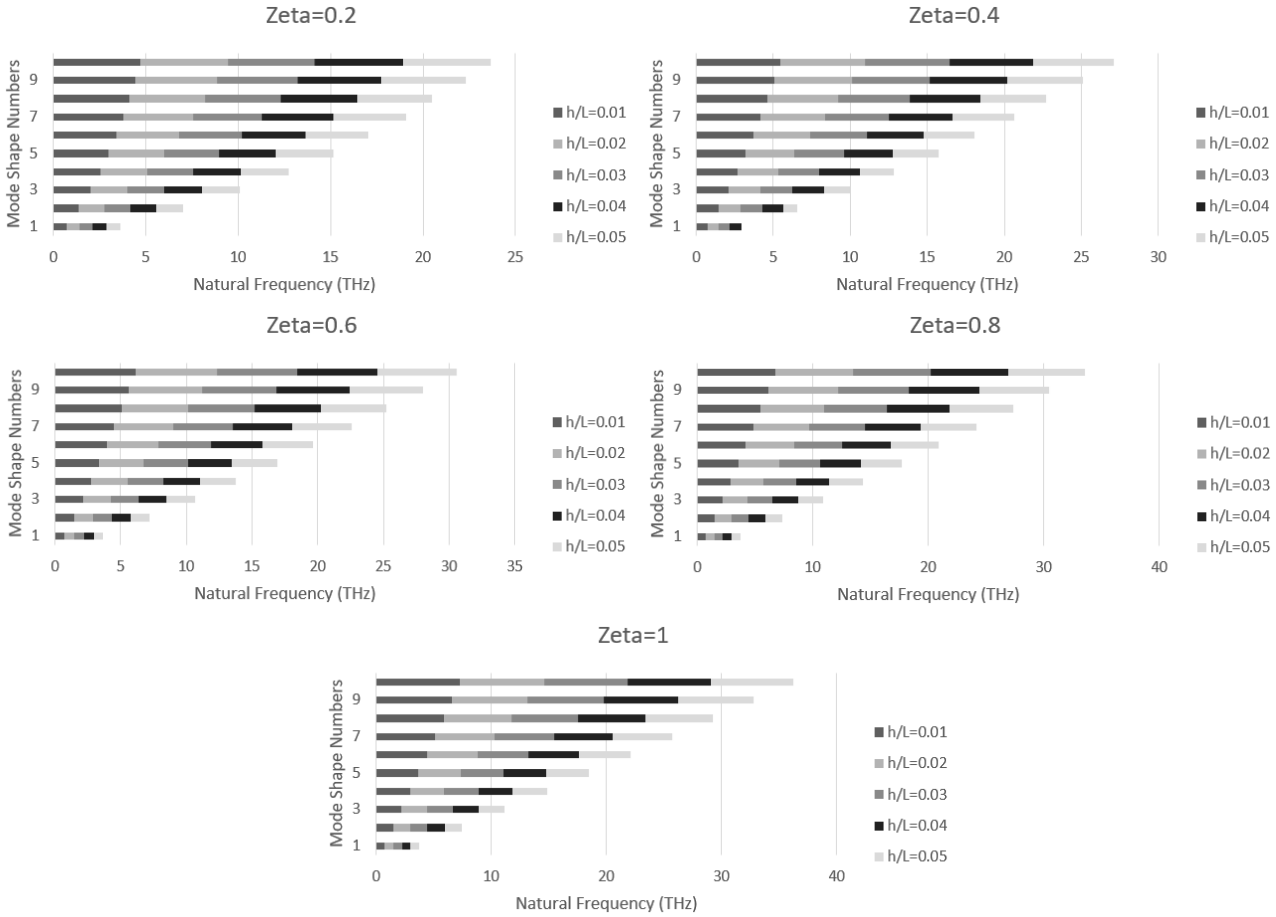

Fig. 2 Natural Frequencies for distinct values of H/L and ζ, κ/L=0.05

contours. All figures below truly illustrated that how related the key parameters which enjoy a key role in final result is. Five first natural frequencies are considered in this part. The first figures devoted to the first natural frequency, and 4 types of ζ are indicated. As demonstrated in Fig. 4, when $\zeta = 1$ from left to right alterations of the first natural frequency are sorted. In addition, it could be mentioned here that in lower orders of *H/L*, a slight uniform pattern is occurred, and the region restricted between 0.03 and 0.05 contains more non-uniformity. Upward and downward trend of natural frequency along *H/L* and κ/L interval are completely describable. For $\zeta = 0.8$ lines are placed in a further distance and lines' slope is decreasing. Similar condition is defineable for $\zeta = 0.6$. In other words, increasing line distance and interpenetration in high values of H, and decreasing line slope are extentable. In fourth

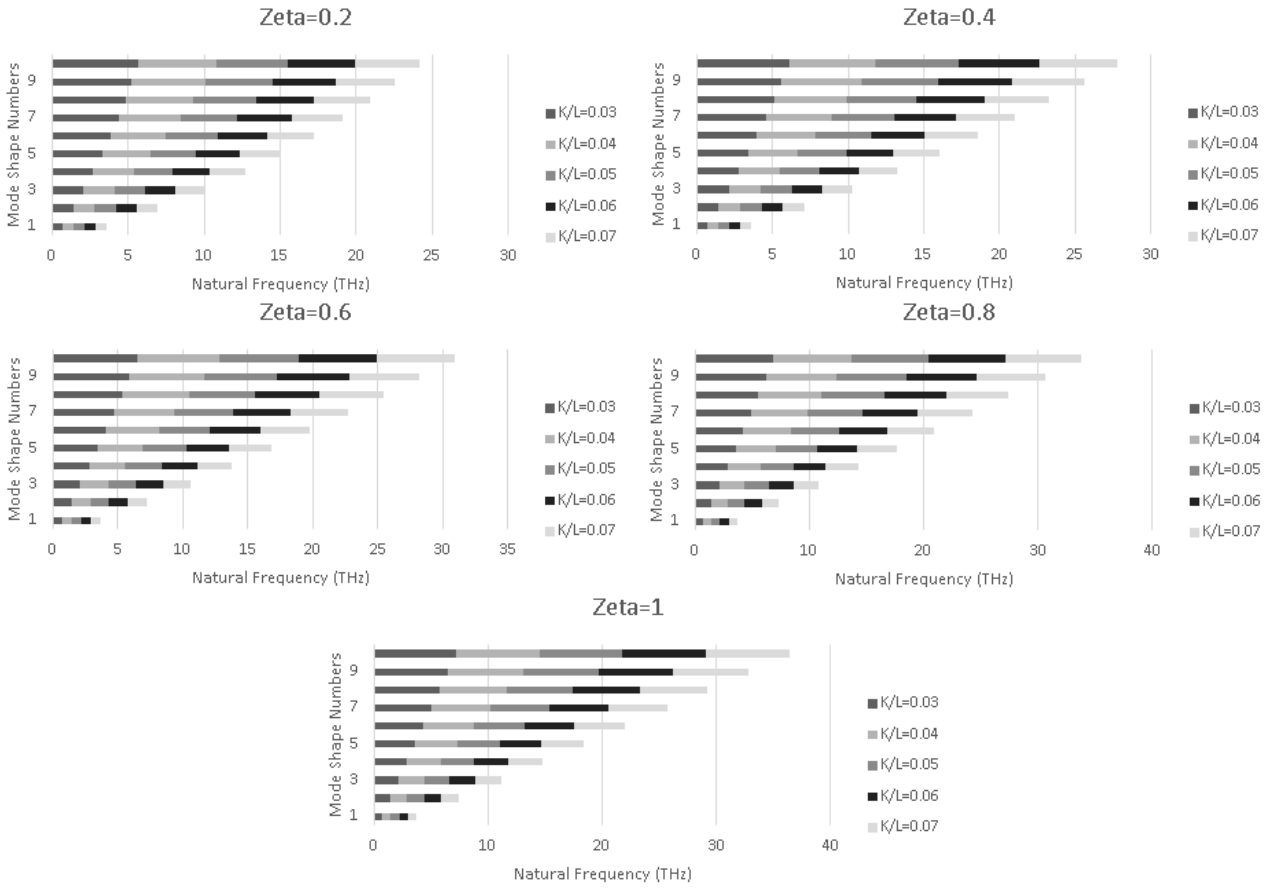

Fig. 3 Natural Frequencies for distinct values of κ/L and ζ, H/L=0.01

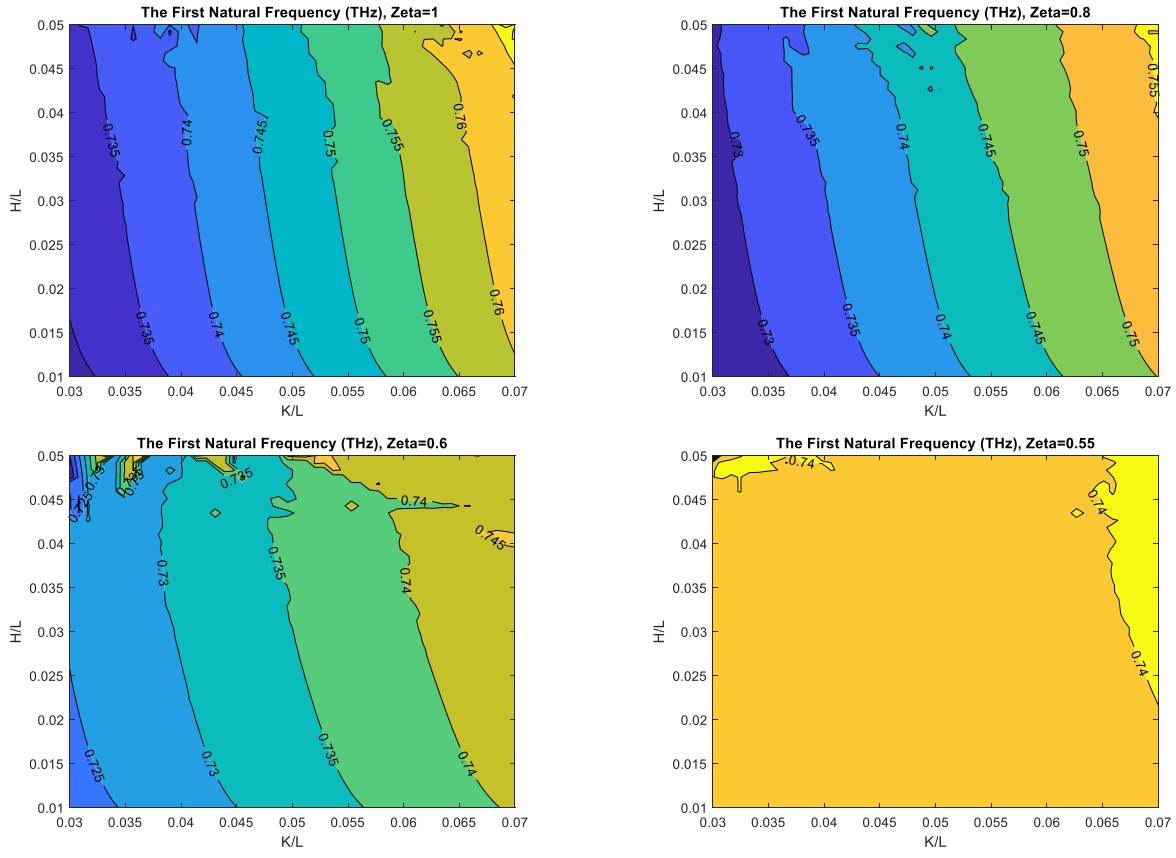

Fig. 4 3D contour of the first natural frequency for distinct values of κ/L, H/L, and ζ

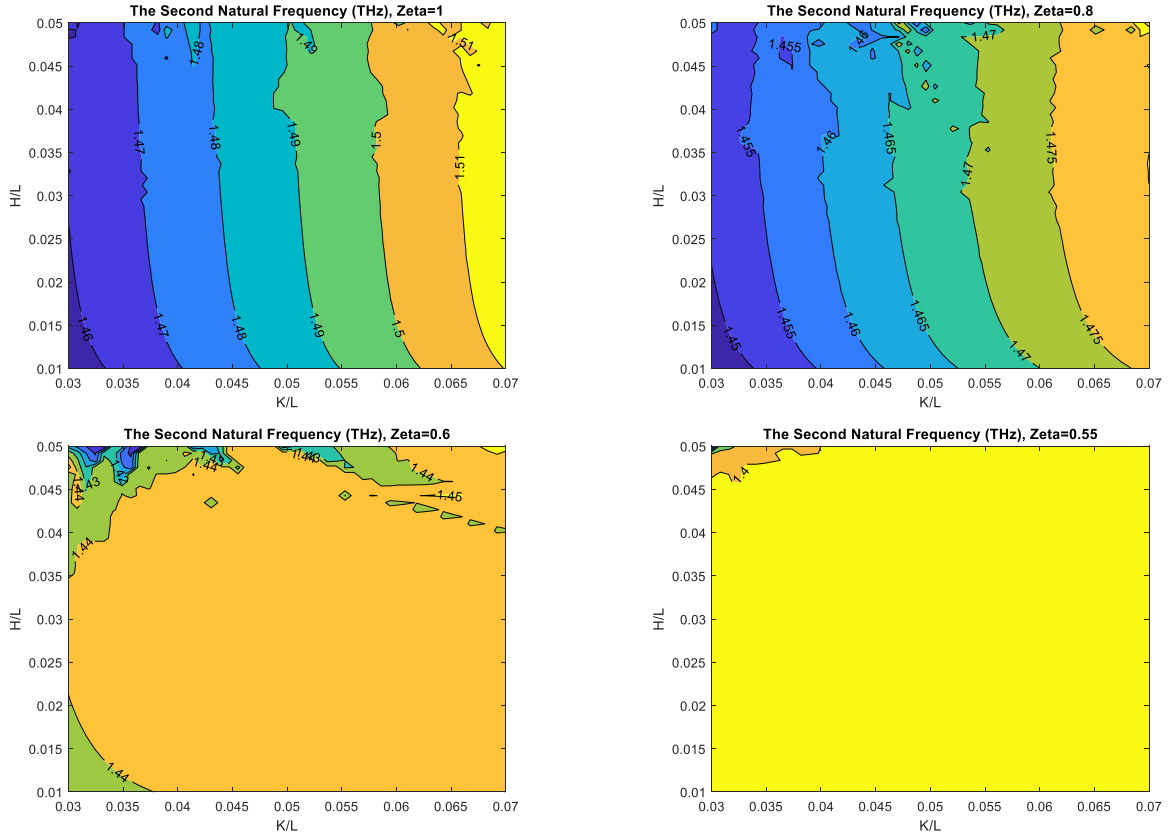

Fig. 5 3D contour of the second natural frequency for distinct values of κ/L, H/L, and ζ

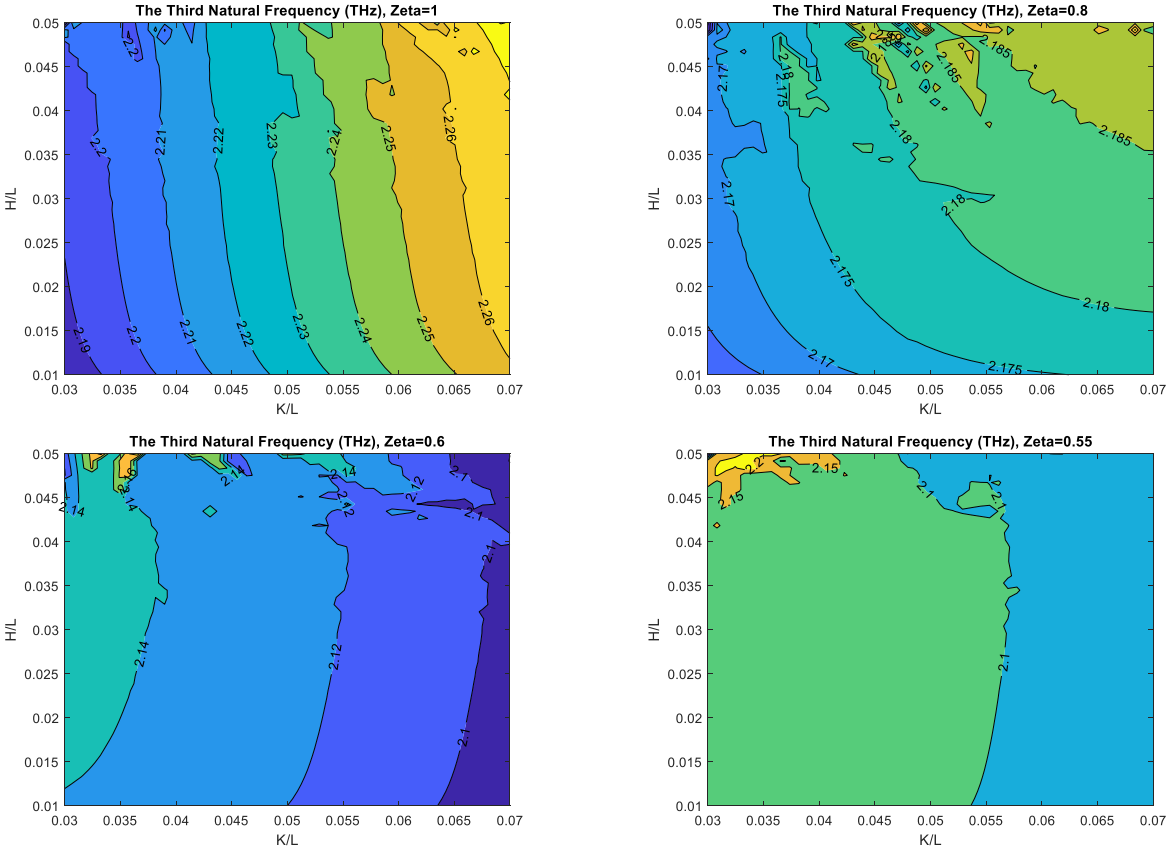

Fig. 6 3D contour of the third natural frequency for distinct values of κ/L, H/L, and ζ

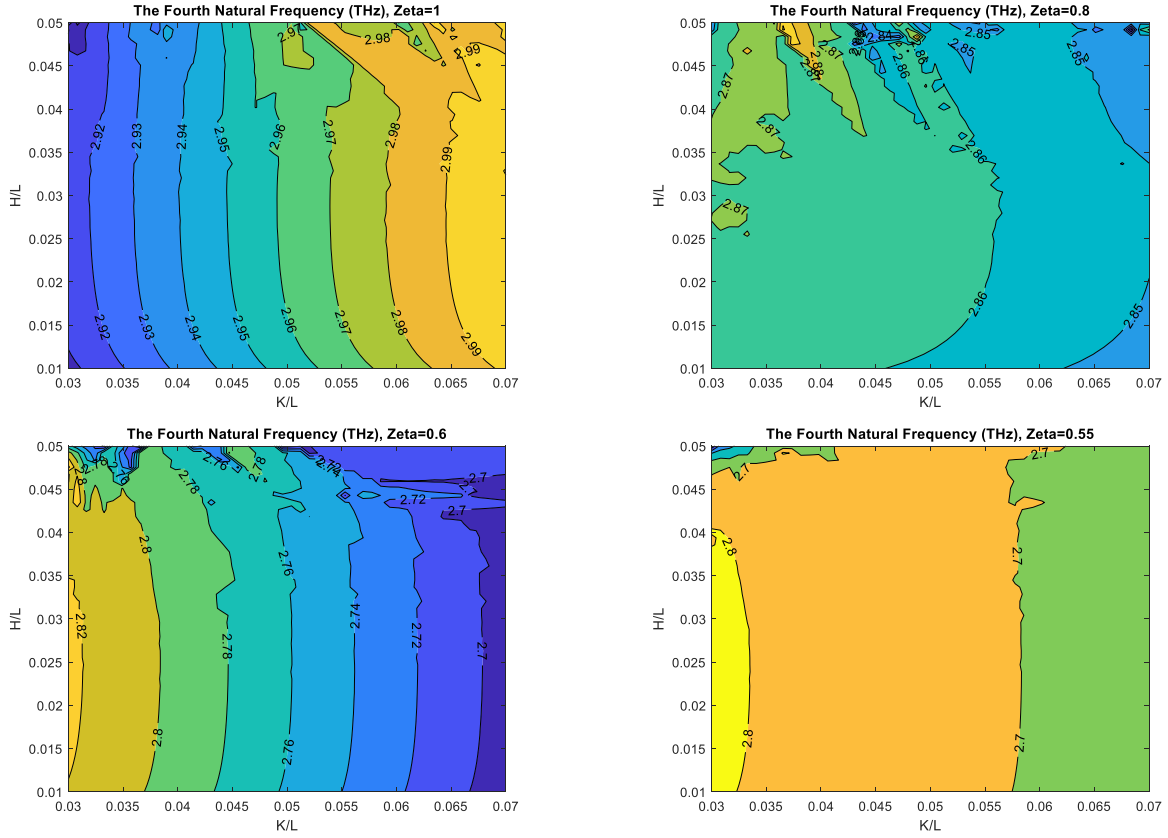

Fig. 7 3D contour of the fourth natural frequency for distinct values of κ/L, H/L, and ζ

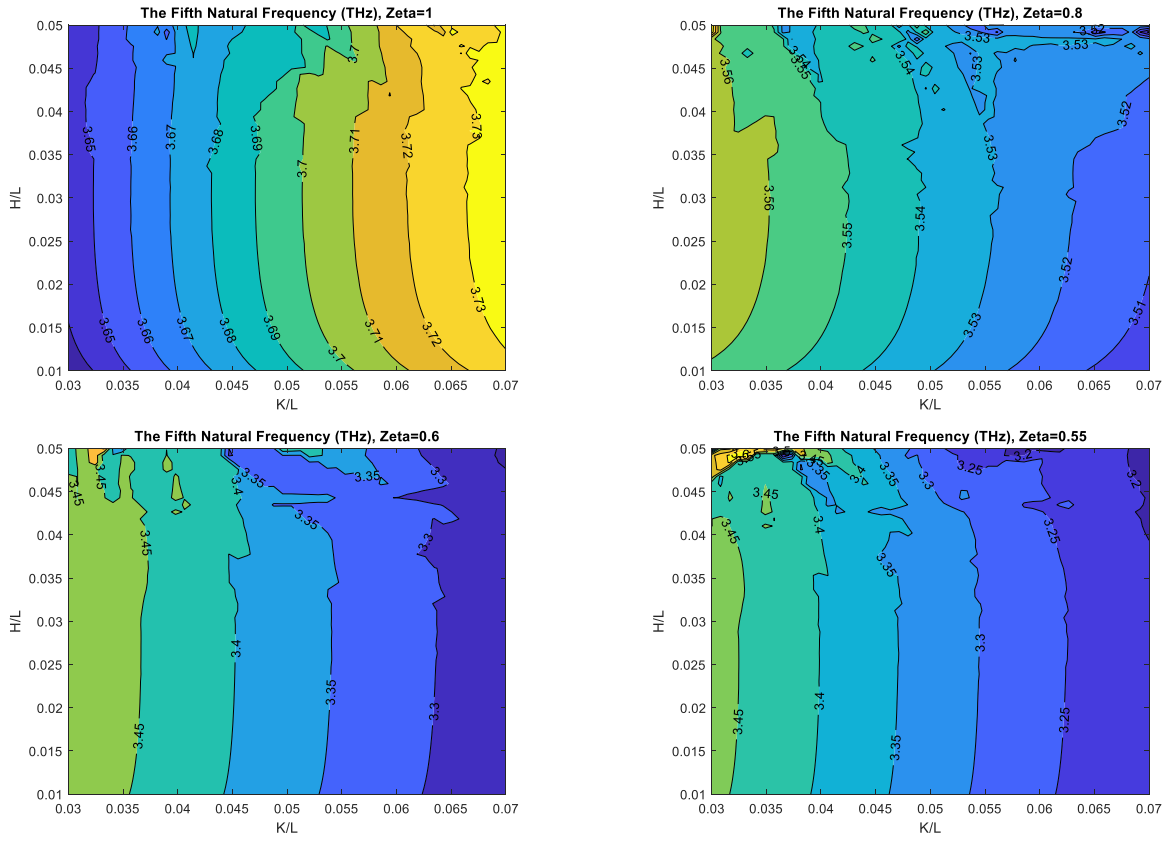

Fig. 8 3D contour of the fifth natural frequency for distinct values of κ/L, H/L, and ζ

section, prior pattern does not exist, and $\zeta = 0.55$ is the minimum number which software was capable to calculate the process, thus the stated value is a brink for local /nonlocal theory in this problem.

For $\zeta = [1, 0.8]$ the condition governed in prior case exists for current case, Fig. 5. Second natural frequency is completely different for $\zeta = 0.6$ since vertical line pattern that governed in the first natural frequency sector change into a circular one, however upper regions remain disorderly. As preceding statement, $\zeta = 0.55$ is the last quantity that software has calculated in this study. This does not result in specific consequence owing to lack of color spectrum. It could be declared that decreasing local phase fraction coefficient cause an intense impact on natural frequency, and omit the diversity of regions.

In Fig. 6, the third natural frequency for $\zeta = 1$ delivers a similar performance like other results described above, but $\zeta = 0.8$ with a circular pattern shows a disorderly form. As mentioned, decreasing approach right to left pattern governs for all prior status, but in this number for $\zeta = 0.6$ being left to right is illusterated. Thus, with decreasing κ/L natural frequency moves towards higher orders. An organized circumstance is definable in Fig. 7 for the fourth natural frequency. In its first part, namely $\zeta = 1$, upper regions remains tangled. A complicated shape is demonstrated for $\zeta = 0.8$, but in next figure if the intricate area can be assumed negligible, it can be stated that an orderly lines is occurred with an inverse direction in comparison with fully local status. It seems that for $\zeta = 0.55$ further diversity exist than prior and lower orders of natural frequency. In other words, more spectrum is shown comparing to other condition. Eventually, the fifth natural frequency as the last case is introduced. It is essential to mention here that distance of lines is less than what is expected, and a smooth pattern is demonstrated for $\zeta = 1$. In this mode shape number, except upper zones neither circular pattern nor disorders exist.

8. Conclusions

Bishop theory has not been utilized by researchers thus far, and there is no such an investigation based on this theory, thus this study concentrates on employing and studying its how compatible with longitudinal vibration of Nano-beams through two phase local/nonlocal theory. Governing equations are derived by means of Hamilton's principle and two-phase local/nonlocal elasticity. To solve the equation, the sixth order Generalized Differential Quadrature Method (GDQM) is employed. A list comprising eminent achievements of this work is defined below

• High accuracy and pace of sixth order GDQM caused a smooth and easy process of numerical calculation.

• Discrepancy of height of cross section in lower case do not produce a significant effect on natural frequency, but for higher order of local phase fraction coefficient, increasing *H/L* cause a noticeable upward moving of natural frequency.

• Reasonable relation of $\zeta = 0.2$ for all κ/L is distinguishable. Except the first natural frequency column rest of columns of natural frequency for each ζ follows a decreasing trend.

• Upward trend of natural frequency from left to right with increasing κ/L for all types of ζ is mentionable, but with increasing natural frequency order a reverse trend is replaced. Hence, just the fifth natural frequency for $\zeta = 1$ enjoys the left to right pattern.

• From 0.03 to 0.05 for *H/L*, the amount of tangled lines is noticeable.

• In upper order of natural frequency more extended solutions are prepared than lower cases. For instance, in the last case for $\zeta = 0.55$ a colorful spectrum of solution are presented.

• The number of 0.55 is a limit in employing two phase local/nonlocal elasticity.

References

Apuzzo, A., Barretta, R., Luciano, R., De Sciarra, F.M. and Penna, R. (2017), "Free vibrations of Bernoulli-Euler nano-beams by the stress-driven nonlocal integral model". *Compos. Part B Eng.*, **123**, 105-111, https://doi.org/10.1016/j.compositesb.2017.03.057

Bergman, R.M. (1968), "Asymptotic analysis of some plane problems of the theory op elasticity with couple stresses". *J. Appl. Math. Mech.*, **32**(6), 1085-1090. https://doi.org/10.1016/0021-8928(68)90035-X

Bert, C.W. and Malik, M. (1996), "Differential quadrature method in computational mechanics: A review", *ASME. Appl. Mech. Rev.*, **49**(1), 1-28. https://doi.org/10.1115/1.3101882

Besseghier, A., Heireche, H., Bousahla, A.A., Tounsi, A. and Benzair, A. (2015), "Nonlinear vibration properties of a zigzag single-walled carbon nanotube embedded in a polymer matrix", *Adv. Nano Res.*, **3**(1), 029. https://doi.org/10.12989/anr.2015.3.1.029

Chaht, F.L., Kaci, A., Houari, M.S.A., Tounsi, A., Bég, O.A. and Mahmoud, S.R. (2015), "Bending and buckling analyses of functionally graded material (FGM) size-dependent nanoscale beams including the thickness stretching effect", *Steel Compos. Struct.*, **18**(2), 425-442. https://doi.org/10.12989/scs.2015.18.2.425

Challamel, N., Zhang, Z., Wang, C.M., Reddy, J.N., Wang, Q., Michelitsch, T. and Collet, B. (2014), "On nonconservativeness of Eringen's nonlocal elasticity in beam mechanics: correction from a discrete-based approach", *Arch. Appl. Mech.*, **84**(9), 1275-1292. https://doi.org/10.1007/s00419-014-0862-x

Civalek, Ö. and Numanoğlu, H.M. (2020), "Nonlocal finite element analysis for axial vibration of embedded love-bishop nanorods", *Int. J. Mech. Sci.*, **188**, 105939. https://doi.org/10.1016/j.ijmecsci.2020.105939

Eltaher, M.A., Emam, S.A. and Mahmoud, F.F. (2012), "Free vibration analysis of functionally graded size-dependent nanobeams", *Applied Math. Comput.*, **218**(14), 7406-7420. https://doi.org/10.1016/j.amc.2011.12.090

Eringen, A.C. (1983), "On differential equations of nonlocal elasticity and solutions of screw dislocation and surface waves", *J. Appl. Phys.*, **54**(9), 4703-4710. https://doi.org/10.1063/1.332803

Eringen, A.C. (1984), "Theory of nonlocal elasticity and some applications", *Res. Mech.*, **21**(4), 313-342. https://doi.org/10.21236/ada145201

Eringen, A.C. and Wegner, J.L. (2003), "Nonlocal continuum field theories", *Appl. Mech. Rev.*, **56**(2), B20-B22.

https://doi.org/10.1115/1.1553434
Fernández-Sáez, J., Zaera, R., Loya, J.A. and Reddy, J. (2016), "Bending of Euler-Bernoulli beams using Eringen's integral formulation: a paradox resolved", *Int. J. Eng. Sci.*, **99**, 107-116. https://doi.org/10.1016/j.ijengsci.2015.10.013
Fleck, N.A., Muller, G.M., Ashby, M.F. and Hutchinson, J.W. (1994), "Strain gradient plasticity: theory and experiment", *Acta Metallurgica et Materialia*, **42**(2), 475-487. https://doi.org/10.1016/0956-7151(94)90502-9
Hosseini, S.A., Khosravi, F. and Ghadiri, M. (2020), "Moving axial load on dynamic response of single-walled carbon nanotubes using classical, Rayleigh and Bishop rod models based on Eringen's theory", *J. Vib. Control*, **26**(11-12), 913-928. https://doi.org/10.1177/1077546319890170
Hsu, J.C., Lee, H.L. and Chang, W.J. (2011), "Longitudinal vibration of cracked nanobeams using nonlocal elasticity theory", *Curr. Appl. Phys.*, **11**(6), 1384-1388. https://doi.org/10.1016/j.cap.2011.04.026
Jalaei, M.H., Thai, H.T. and Civalek, Ö. (2022), "On viscoelastic transient response of magnetically imperfect functionally graded nanobeams", *Int. J. Eng. Sci.*, **172**, 103629. https://doi.org/10.1016/j.ijengsci.2022.103629
Khaniki, H.B. (2018), "On vibrations of nanobeam systems", *Int. J. Eng. Sci.*, **124**, 85-103. https://doi.org/10.1016/j.ijengsci.2017.12.010
Lam, D.C., Yang, F., Chong, A.C.M., Wang, J. and Tong, P. (2003), "Experiments and theory in strain gradient elasticity", *J. Mech. Phys. Solids*, **51**(8), 1477-1508. https://doi.org/10.1016/S0022-5096(03)00053-X
Lei, Y., Adhikari, S. and Friswell, M.I. (2013), "Vibration of nonlocal Kelvin-Voigt viscoelastic damped Timoshenko beams", *Int. J. Eng. Sci.*, **66**, 1-13. https://doi.org/10.1016/j.ijengsci.2013.02.004
Li, H.B. and Wang, X. (2012), "Effect of small scale on the dynamic characteristic of carbon nanotubes under axially oscillating loading", *Physica E*, **46**, 198-205. https://doi.org/10.1016/j.physe.2012.09.015
Lim, C.W., Zhang, G. and Reddy, J. (2015), "A higher-order nonlocal elasticity and strain gradient theory and its applications in wave propagation", *J. Mech. Phys. Solids*, **78**, 298-313. https://doi.org/10.1016/j.jmps.2015.02.001
Lin, F., Tong, L.H., Shen, H.S., Lim, C.W. and Xiang, Y. (2020), "Assessment of first and third order shear deformation beam theories for the buckling and vibration analysis of nanobeams incorporating surface stress effects", *Int. J. Mech. Sci.*, **186**, 105873. https://doi.org/10.1016/j.ijmecsci.2020.105873
Lu, L., Guo, X. and Zhao, J. (2017), "A unified nonlocal strain gradient model for nanobeams and the importance of higher order terms". *Int. J. Eng. Sci.*, **119**, 265-277. https://doi.org/10.1016/j.ijengsci.2017.06.024
Mashat, D.S., Zenkour, A.M. and Sobhy, M. (2016), "Investigation of vibration and thermal buckling of nanobeams embedded in an elastic medium under various boundary conditions", *J. Mech.*, **32**(3), 277-287. https://doi.org/10.1017/jmech.2015.83
Mirafzal, A. and Fereidoon, A. (2017), "Dynamic characteristics of temperature-dependent viscoelastic FG nanobeams subjected to 2D-magnetic field under periodic loading", *Appl. Phys. A*, **123**(4), 1-13. https://doi.org/10.1007/s00339-017-0829-1
Naderi, A., Behdad, S., Fakher, M. and Hosseini-Hashemi, S. (2020), "Vibration analysis of mass nanosensors with considering the axial-flexural coupling based on the two-phase local/nonlocal elasticity", *Mech. Syst. Signal Pr.*, **145**, 106931. https://doi.org/10.1016/j.ymssp.2020.106931
Nazemnezhad, R. and Kamali, K. (2018), "Free axial vibration analysis of axially functionally graded thick nanorods using nonlocal Bishop's theory", *Steel Compos. Struct.*, **28**(6), 749-758. https://doi.org/10.12989/scs.2018.28.6.749
Nazemnezhad, R. and Shokrollahi, H. (2022), "Axial frequency analysis of axially functionally graded Love-Bishop nanorods using surface elasticity theory", *Steel Compos. Struct.*, **42**(5), 699-710. https://doi.org/10.12989/scs.2022.42.5.699
Numanoğlu, H.M. and Civalek, Ö. (2019), "On the torsional vibration of nanorods surrounded by elastic matrix via nonlocal FEM", *Int. J. Mech. Sci.*, **161**, 105076. https://doi.org/10.1016/j.ijmecsci.2019.105076
Numanoğlu, H.M. and Civalek, Ö. (2022), "Novel size-dependent finite element formulation for modal analysis of cracked nanorods", *Materials Today Commun.*, **31**, 103545. https://doi.org/10.1016/j.mtcomm.2022.103545
Numanoğlu, H.M., Akgöz, B. and Civalek, Ö. (2018), "On dynamic analysis of nanorods", *Int. J. Eng. Sci.*, **130**, 33-50. https://doi.org/10.1016/j.ijengsci.2018.05.001
Numanoğlu, H.M., Ersoy, H., Akgöz, B. and Civalek, Ö. (2022), "A new eigenvalue problem solver for thermo-mechanical vibration of Timoshenko nanobeams by an innovative nonlocal finite element method", *Math. Method Appl. Sci.*, **45**(5), 2592-2614. https://doi.org/10.1002/mma.7942
Polyanin, A.D. and Manzhirov, A.V. (2008), Handbook of Integral Equations, Chapman and Hall/CRC.
Quan, J.R. and Chang, C.T. (1989), "New insights in solving distributed system equations by the quadrature method—I. Analysis", *Comput. Chem. Eng.*, **13**(7), 779-788. https://doi.org/10.1016/0098-1354(89)85051-3
Rao, S.S. (2019), *Vibration of Continuous Systems*, John Wiley & Sons.
Reddy, J. (2007), "Nonlocal theories for bending, buckling and vibration of beams", *Int. J. Eng. Sci.*, **45**(2-8), 288-307. https://doi.org/10.1016/j.ijengsci.2007.04.004
Shafiei, N., Mirjavadi, S.S., Afshari, B.M., Rabby, S. and Hamouda, A.M.S. (2017), "Nonlinear thermal buckling of axially functionally graded micro and nanobeams", *Comp. Struct.*, **168**, 428-439. https://doi.org/10.1016/j.compstruct.2017.02.048
Shen, Y., Chen, Y. and Li, L. (2016), "Torsion of a functionally graded material", *Int. J. Eng. Sci.*, **109**, 14-28. https://doi.org/10.1016/j.ijengsci.2016.09.003
Shu, C. and Richards, B.E. (1992), "Application of generalized differential quadrature to solve two-dimensional incompressible Navier-Stokes equations", *Int. J. Numer. Method Fluids*, **15**(7), 791-798. https://doi.org/10.1002/fld.1650150704
Şimşek, M. and Yurtcu, H.H. (2013), "Analytical solutions for bending and buckling of functionally graded nanobeams based on the nonlocal Timoshenko beam theory", *Comp. Struct.*, **97**, 378-386. https://doi.org/10.1016/j.compstruct.2012.10.038
Thai, H.T. (2012), "A nonlocal beam theory for bending, buckling, and vibration of nanobeams", *Int. J. Eng. Sci.*, **52**, 56-64. https://doi.org/10.1016/j.ijengsci.2011.11.011
Wang, Y., Zhao, Y.B. and Wei, G.W. (2003), "A note on the numerical solution of high-order differential equations", *J. Comput. Appl. Math.*, **159**(2), 387-398. https://doi.org/10.1016/S0377-0427(03)00541-7
Wang, Y.B., Zhu, X.W. and Dai, H.H. (2016), "Exact solutions for the static bending of Euler-Bernoulli beams using Eringen's two-phase local/nonlocal model", *Aip Adv.*, **6**(8), 085114. https://doi.org/10.1063/1.4961695
Wu, T.Y. and Liu, G.R. (2000), "Application of generalized differential quadrature rule to sixth-order differential equations", *Commun. Numer. Methods Eng.*, **16**(11), 777-784. https://doi.org/10.1002/10990887(200011)16:11<777::AID-CNM375>3.0.CO;2-6
Wu, T.Y. and Liu, G.R. (2001), "Free vibration analysis of circular plates with variable thickness by the generalized differential quadrature rule", *Int. J. Solids Struct.*, **38**(44-45), 7967-7980. https://doi.org/10.1016/S0020-7683(01)00077-4

Zhang, G.Y. and Gao, X.L. (2020), "A new Bernoulli-Euler beam model based on a reformulated strain gradient elasticity theory", *Math. Mech. Solids*, **25**(3), 630-643. https://doi.org/10.1177/1081286519886003

Zhang, G.Y., Gao, X.L., Zheng, C.Y. and Mi, C.W. (2021), "A non-classical Bernoulli-Euler beam model based on a simplified micromorphic elasticity theory", *Mech. Mater.*, **161**, 103967. https://doi.org/10.1016/j.mechmat.2021.103967

Zhao, X., Zheng, S. and Li, Z. (2020), "Effects of porosity and flexoelectricity on static bending and free vibration of AFG piezoelectric nanobeams", *Thin Walled Struct.*, **151**, 106754. https://doi.org/10.1016/j.tws.2020.106754

Zhu, X. and Li, L. (2017), "Twisting statics of functionally graded nanotubes using Eringen's nonlocal integral model", *Compos. Struct.*, **178**, 87-96. https://doi.org/10.1016/j.compstruct.2017.06.067

Zhu, X., Wang, Y. and Dai, H.H. (2017), "Buckling analysis of Euler-Bernoulli beams using Eringen's two-phase nonlocal model", *Int. J. Eng. Sci.*, **116**, 130-140. https://doi.org/10.1016/j.ijengsci.2017.03.008

CC

Appendix

$$\begin{cases} a_{10} = \left(l_1^{(1)}(x_1) + \dfrac{2}{x_1 - x_N}\right)^2 - \dfrac{l_1^{(2)}(x_1)}{2} - \dfrac{1}{(x_1 - x_N)^2} - \dfrac{2l_1^{(1)}(x_1)}{x_1 - x_N} \\ a_{11} = -\left(l_1^{(1)}(x_1) + \dfrac{2}{x_1 - x_N}\right) \\ a_{12} = \dfrac{1}{2} \end{cases}$$

$$\begin{cases} b_{10} = -\left(l_1^{(1)}(x_1) + \dfrac{2}{x_1 - x_N}\right) - 2x_1 a_{10} \\ b_{11} = 1 - 2x_1 a_{11} \\ b_{12} = -x_1 \end{cases}$$

$$\begin{cases} c_{10} = x_1\left(l_1^{(1)}(x_1) + \dfrac{2}{x_1 - x_N}\right) + {x_1}^2 a_{10} + 1 \\ c_{11} = x_1(x_1 a_{11} - 1) \\ c_{12} = \dfrac{{x_1}^2}{2} \end{cases}$$

$$\begin{cases} a_{N0} = \left(l_N^{(1)}(x_N) - \dfrac{2}{x_1 - x_N}\right)^2 - \dfrac{l_N^{(2)}(x_N)}{2} - \dfrac{1}{(x_1 - x_N)^2} + \dfrac{2l_N^{(1)}(x_N)}{x_1 - x_N} \\ a_{N1} = -\left(l_N^{(1)}(x_N) - \dfrac{2}{x_1 - x_N}\right) \\ a_{N2} = \dfrac{1}{2} \end{cases}$$

$$\begin{cases} b_{N0} = -\left(l_N^{(1)}(x_N) - \dfrac{2}{x_1 - x_N}\right) - 2x_N a_{N0} \\ b_{N1} = 1 - 2x_N a_{N1} \\ b_{N2} = -x_N \end{cases}$$

$$\begin{cases} c_{N0} = x_N\left(l_N^{(1)}(x_N) - \dfrac{2}{x_1 - x_N}\right) + {x_N}^2 a_{N0} + 1 \\ c_{N1} = x_N(x_N a_{N1} - 1) \\ c_{N2} = \dfrac{{x_N}^2}{2} \end{cases}$$